

J-complexes of retinol formed within the nanoparticles prepared from microemulsions

C. Destrée · S. George · B. Champagne · M. Guillaume · J. Ghijsen · J. B. Nagy

Received: 16 February 2007 / Accepted: 25 March 2007 / Published online: 13 June 2007
© Springer-Verlag 2007

Abstract Retinol nanoparticles have been obtained by direct precipitation of retinol in the inner water cores of AOT/heptane/water microemulsions. The retinol dissolved in chloroform was injected into the microemulsion. The diameter of the so-obtained nanoparticles was measured using transmission electron microscope pictures where the revelation was made thanks to adsorbed iodine on the nanoparticles. The size is ca 6.0 nm, and it is not dependent either on the size of the water droplets or the concentration of the retinol molecules. This phenomenon is explained by the thermodynamic stabilization of the nanoparticles at a certain size. UV-visible spectra of the nanoparticles show a new band the maximum of which has a bathochromic shift with respect to the absorption band of the retinol monomers. If the bathochromic shift is plotted as a function of the line width, a linear correlation is obtained, the line width is decreasing with increasing shift. This behavior is interpreted as being due to an excitonic transition of a J-complex. Quantum chemical calculations have been carried

out to confirm the presence of J-complexes. Taking into account the various possible geometries, the results confirm the presence of J-complexes composed of three head-to-tail molecules on the average.

Keywords Nanoparticles · Microemulsions

Introduction

Among the various methods known for the preparation of the monodisperse nanoparticles, we prefer the mild conditions linked to the use of microemulsions [1, 2]. Indeed, the synthesis of nanoparticles in microemulsions allows one to obtain particles of monodisperse size and to control the size by variation of the size of the microemulsion droplet radius and of the precursor concentrations.

For a quantitative evaluation of the properties of colloidal dispersions, the monodisperse nature—uniform in size and in shape—is a prerequisite. The quantum size effects are particularly studied, as they lead to interesting mechanical, chemical, electrical, optical, electro-optical, and magneto-optical properties which are quite different from those reported for bulk materials [1, 3–5].

In particular, the unique optical properties due to dimensionality and discreteness induced by the confinement of these nanostructured materials deserve much attention [6]. For example, dye aggregates play an important role in many technological applications. Due to their strong light absorption, they are used for spectral sensitization of the photographic process with silver halides and may be considered for future light harvesting systems [6–11].

In this paper, we focus our attention on the preparation of nanoparticles of retinol prepared from AOT/heptane/

C. Destrée · S. George · J. B. Nagy (✉)
Laboratoire de RMN,
Facultés Universitaires Notre-Dame de la Paix,
61 rue de Bruxelles,
5000 Namur, Belgium
e-mail: janos.bnagy@fundp.ac.be

B. Champagne · M. Guillaume
Laboratoire CTA,
Facultés Universitaires Notre-Dame de la Paix,
61 rue de Bruxelles,
5000 Namur, Belgium

J. Ghijsen
Laboratoire LISE,
Facultés Universitaires Notre-Dame de la Paix,
61 rue de Bruxelles,
5000 Namur, Belgium

water microemulsions. We show the formation of J-complexes by UV-visible spectroscopy. The quantum chemical computations confirm the existence of these J-complexes. Details concerning the formation of J-complexes by dyes deposited on silver halide nanoparticles will be added, when necessary, for the general argumentation.

Experimental

Description of the microemulsion

The AOT/heptane/water ternary diagram is illustrated in Fig. 1. It can be seen that the microemulsion exists over a large domain (L_2 in Fig. 1). AOT or sodium bis-(2-ethylhexyl) sulfosuccinate is an anionic surfactant.

Materials

The two molecules, cholesterol, and retinol are represented in Fig. 1. Their origin, together with that of all the substances studied, are: cholesterol (95%, Sigma-Aldrich); retinol (95%, Sigma Aldrich); heptane [99%, high-performance liquid chromatography (HPLC) grade, Sigma-Aldrich]; AOT (Sigma-Aldrich); water milli Q (18.2 m Ω /cm); chloroform (99%, stabilized with 0.75% ethanol, Jansen Chemica); iodine (resublimated, Riedel-de-Haën); silica gel (60, HPLC, Merck).

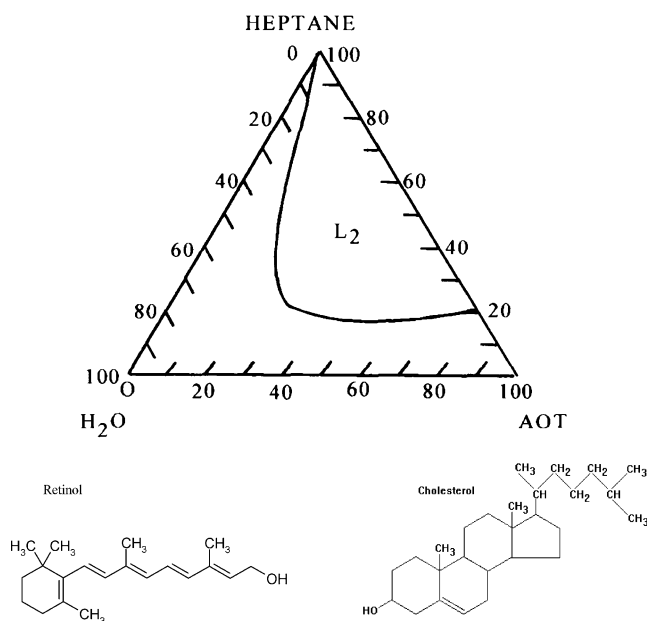


Fig. 1 Ternary diagram of AOT/heptane/water system (the large domain L_2 shows the existence of microemulsion) and molecular structures of cholesterol and retinol

General method of preparation of organic nanoparticles

The synthesis of organic nanoparticles consists in precipitating them directly in the water cores of the microemulsion [12]. The experimental procedure is:

- Dissolve AOT in heptane (0.12 M).
- Add the desired amount of water for achieving a particular $R=[H_2O]/[surfactant]$ ratio.
- Treat the mixture under ultrasound until a limpid solution is obtained.
- Add the solution of the active principle (cholesterol or retinol) in chloroform drop by drop or using a syringe.
- Treat the system under ultrasound during 15 min.

Revelation of the organic nanoparticles

The organic nanoparticles prepared in the microemulsion are deposited on a metallic grid, of 3 mm of diameter, having a rhodium and a copper face. The rhodium face is covered by a vinyl polymer, formvar, to facilitate the adhesion of the particles on the grid.

Iodine was essentially used as a contrasting agent. Iodine, adsorbed on silica, is placed in a closed system, and the grids are put in HPLC tubes to allow depositing iodine by sublimation.

The transmission electron microscope (TEM) pictures were taken on a Philips Tecnai 10 electron microscope.

Finally, the photographs were analyzed by Adobe Photoshop and Global Lab systems that allow one to measure automatically the size of the particles and to construct the histograms.

2H -NMR measurements

The 2H -NMR spectra of deuterated compounds were taken on an MSL 400 Bruker spectrometer. For 2H ($\nu=61.4$ MHz), a 5.0- μ s pulse was used ($\theta=\pi/10$) together with a repetition time of 1.0 s [10].

Quantum chemical computation

The semi-empirical ZINDO method was used to compute the optical properties of conjugated organic molecules [13, 14]. This method was already successfully used to simulate the UV-visible absorption spectra of the aggregates formed by 2-methyl-4-nitroaniline [15] and by 3-methyl-4-nitropyridine-1-oxide [16]. This approximation is based on the technique of configuration interaction (CI), including singly excited Slater determinants combined with the semi-empirical Zerner's INDO/S parameterization. The repulsion integrals are computed with the help of Nishimoto–Mataga–Weiss expression, $k=1.0$, $f=1.2$.

The determination of the excited states and their properties was carried out including in the CI space a number of occupied and unoccupied molecular orbitals equal to ten times the number of retinol molecules in the aggregate (10 n). This allows one to reduce at the maximum errors associated with size inconstancy while maintaining a reasonable time of computation even for the largest aggregates. These simulations were carried out using the semi-empirical molecular orbital package for spectroscopy (MOSF 4.2 software, Fujitsu V4).

The ZINDO computations yield the wave function and energies for 100 n^2 excited electronic states, and hence, the energies of excitation and the transition dipole moments. Finally, the oscillator strength, proportional to the absorption band intensity, is determined. The spectra are then simulated by associating to each transition a Gaussian function of full width at half maximum (FWHM)=0.3 eV, and the intensity of which is proportional to the oscillator strength.

Results and discussion

Preparation of organic nanoparticles

The nanoparticles of retinol synthesized in the AOT (5.34 wt%)/heptane (92.07 wt%)/water (2.59 wt%) microemulsion are illustrated in Fig. 2, which also contains the corresponding histogram.

To gain a deeper insight into the mechanism of formation of the nanoparticles, the number of nanoparticles per water core has been computed as follows.

The volume of the water core is given by:

$$V_{wc} = \frac{4}{3} \pi r^3$$

where r , the radius of the water core, is computed from the correlation [17]:

$$r(\text{nm}) = 0.18R + 0.45$$

where $R = \frac{[H_2O]}{[AOT]}$

The number of water cores is obtained by dividing the total water volume (V_t) by the volume of a water core:

$$N_{wc} = \frac{V_t}{V_{wc}}$$

In this hypothesis, the amount of water in the organic phase and in the surfactant layer is assumed to be negligible.

On the other hand, the volume of a nanoparticle is obtained from the TEM data $V_{np} = \frac{4}{3} \pi r_{np}^3$. If one can suppose that the density of a nanoparticle is equal to that of the macroscopic material—this hypothesis could be, how-

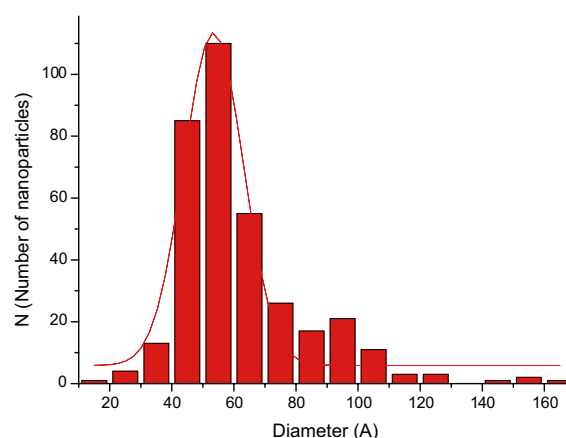
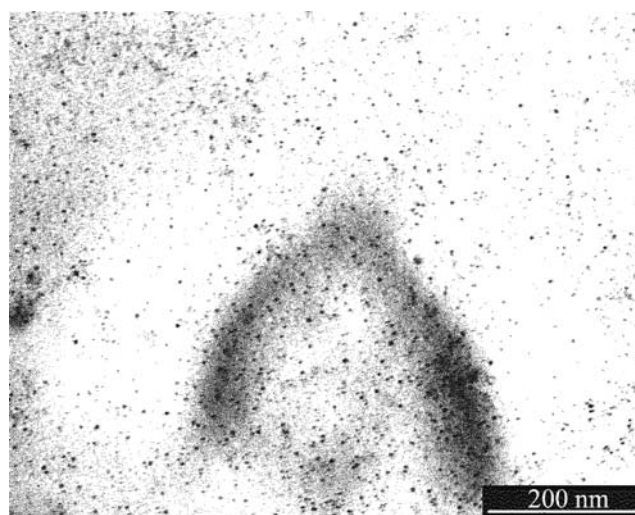


Fig. 2 Photograph of retinol nanoparticles synthesized in AOT/heptane/water microemulsions and the corresponding histogram

ever, questioned—the mass of a single nanoparticle is equal to $m_{np} = V_{np} \times d$, with $d = 1.02$ for retinol [18]. Finally, the number of nanoparticles is given by:

$$N_{np} = \frac{m_t}{m_{np}}$$

where m_t is the total mass of retinol introduced into the microemulsion. In that respect, the very small amount of substance dissolved in water and in the organic phase is neglected.

The number of nanoparticles per water core is given by:

$$N_{np/wc} = \frac{N_{np}}{N_{wc}}$$

To study the influence of R on the size of nanoparticles and $N_{np/wc}$, one has to take into account that the amount of the active principle increases with increasing water content. To eliminate the influence of the concentration of the active

principle, the $N_{\text{np/wc}}$ values have to be normalized to the same concentration of active principle. This is carried out by multiplying $N_{\text{np/wc}}$ by the ratio $V(R=4)/V(R=x)$ where $V(R=x)$ is the volume corresponding to $R=x$ (note that in the figures, the ratio of volumes has been dropped for the sake of simplicity).

Table 1 illustrates the values computed such as the number of water cores, the number of nanoparticles per water core, and finally, the number of retinol molecules per nanoparticle when their diameter is known. Figure 3 shows the variation of the size of the retinol nanoparticles as a function of R and of the concentration of retinol. The size of the nanoparticles varies between 4.0 and 10.0 nm and does not show any presence of a clear-cut minimum, as it was the case for cholesterol nanoparticles [12].

Figure 4 illustrates the variation of $N_{\text{np/wc}}$ as a function of R for various concentrations of retinol. First of all, let us note that $N_{\text{np/wc}}$ values are small and vary from 0.0003 to 0.19. It can be seen that they increase monotonously with increasing R values.

Mechanism of synthesis of nanoparticles in microemulsions

The aqueous droplets continuously collide, coalesce, and break apart, resulting in a continuous exchange of solution content. In fact, the half-life of the exchange reaction between the droplets is of the order of 10^{-3} to 10^{-2} s [19, 20].

Two models have been proposed to explain the size variation of the particles with the precursor concentration

and with the size of the aqueous droplets. The first is based on the LaMer diagram [21, 22] which has been proposed to explain the precipitation in an aqueous medium, and thus, is not specific to the microemulsion. This diagram (Fig. 5) illustrates the variation of the concentration with time during a precipitation reaction and is based on the principle that nucleation is the limiting step in the precipitation reaction. In the first step, the concentration increases continuously with increasing time. As the concentration reaches the critical supersaturation value, nucleation occurs. This leads to a decrease in the concentration. Between the concentrations C_{max}^* and C_{min}^* , nucleation occurs. Later, the decrease in the concentration is due to the growth of the particles by diffusion. This growth occurs until the concentration reaches the solubility value.

This model has been applied to the microemulsion medium, i.e., that nucleation occurs in the first part of the reaction and later, only growth of the particles occurs. If this model is followed, the size of the particles will increase continuously with the concentration of the precursor, or a minimum in the variation of the size with the concentration can also be expected [23]. This stems from the fact that the number of nuclei is constant and the increase in concentration leads to an increase in the size of the particles.

The second model is based on the thermodynamic stabilization of the particles. In this model, the particles are thermodynamically stabilized by the surfactant. The size of the particles stays constant when the precursor concentration and the size of the aqueous droplets vary. In this case, the nucleation occurs continuously during the formation of nanoparticles. The thermodynamic stabilization of a

Table 1 Various parameters characterizing the retinol nanoparticles

| R | Number of retinol molecules ^a | Number of water cores | Number of retinol molecules per water core | Diameter of the particles (Å) | Number of particles per water core | Number of molecules per particle |
|--|--|-----------------------|--|-------------------------------|------------------------------------|----------------------------------|
| Concentration of retinol=10 g/l ^b | | | | | | |
| 4 | 5.41E+17 | 3.86E+18 | 0.14 | 56±14 | 0.00072 | 197.0 |
| 8 | 1.08E+18 | 1.83E+18 | 0.59 | 57±07 | 0.0028 | 207.7 |
| 12 | 1.62E+18 | 1.04E+18 | 1.55 | 57±09 | 0.0075 | 207.7 |
| 30 | 4.06E+18 | 2.32E+17 | 17.5 | 82±35 | 0.028 | 618.5 |
| Concentration of retinol=20 g/l | | | | | | |
| 4 | 1.08E+18 | 3.86E+18 | 0.28 | 95±31 | 0.00029 | 961.8 |
| 8 | 2.16E+18 | 1.83E+18 | 1.18 | 53±21 | 0.0069 | 170.8 |
| 12 | 3.24E+18 | 1.04E+18 | 3.11 | 53±23 | 0.019 | 167.0 |
| 30 | 8.11E+18 | 2.32E+17 | 35.0 | 55±26 | 0.19 | 186.6 |
| Concentration of retinol=40 g/l | | | | | | |
| 4 | 2.16E+18 | 3.86E+18 | 0.56 | 44±15 | 0.0050 | 112.1 |
| 8 | 4.32E+18 | 1.83E+18 | 2.36 | 86±32 | 0.0029 | 807.0 |
| 12 | 6.49E+18 | 1.04E+18 | 6.21 | 56±15 | 0.035 | 176.6 |
| 30 | 1.62E+19 | 2.32E+17 | 69.9 | 70±22 | 0.18 | 384.8 |

^a In 5.0 ml of solution

^b The concentration is given with respect to chloroform.

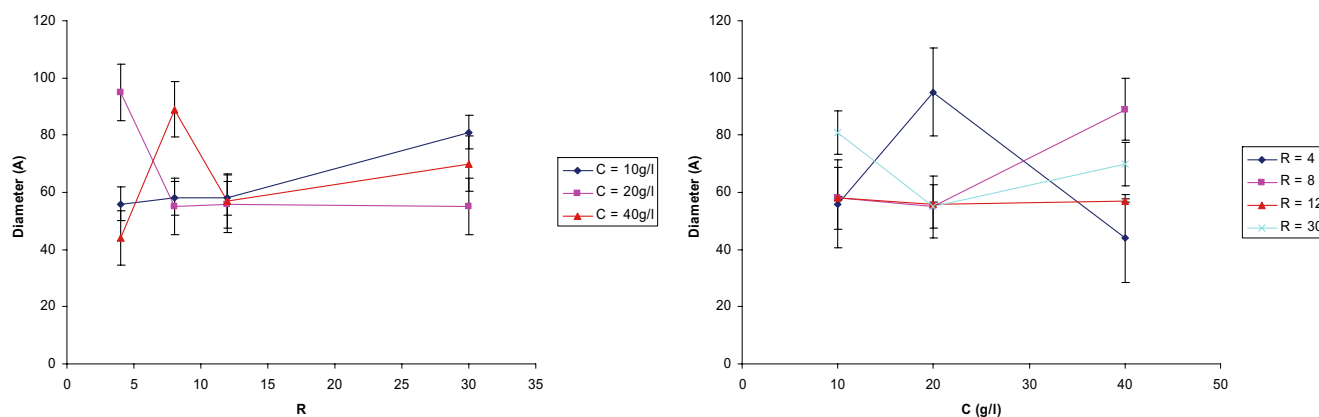


Fig. 3 Variation of the size of the retinol nanoparticles as a function of R ($R = \frac{[\text{water}]}{[\text{surfactant}]}$) and of the concentration of retinol (C in g/l)

certain size of the nanoparticle is nicely demonstrated by the formation of ZrO_2 in aqueous media. Primary particles—crystalline needles—are formed first that coagulate under the influence of carboxylic acids of various lengths, leading to the formation of monodisperse nanoparticles the size of which is governed by the nature and concentration of the carboxylic acid [24].

These two models are limiting models; the LaMer diagram does not take into account the stabilization of the particles by the surfactant, and the thermodynamic stabilization model does not take into account that the nucleation of the particles is more difficult than the growth by diffusion.

Obviously, when the particle size passes through a minimum as a function of R , this is the case of cholesterol, the model of LaMer is playing a role, that is, the slow nucleation governs the number of the first nuclei that grow until the exhaustion of the nutrient [25]. On the other hand, when the size of the nanoparticles remains constant as a function of either R or the initial concentration of the

organic molecules, the thermodynamic control is favoring a certain size of the nanoparticles.

Finally, a model can explain the formation of organic nanoparticles by direct precipitation in the inner water cores of the microemulsion (Fig. 6).

The retinol dissolved in the good vector solvent (chloroform) is transported through the organic medium and the interface formed by the surfactants (2°). The nucleus formed is a molecule of retinol stabilized at the interface by the interaction with the surfactant molecules (3°). The fast exchange (10^{-3} – 10^{-2} s) between the water cores brings other organic molecules, and the nanoparticle is formed (4°). The growth can come from either collision between micelles or from isolated molecules coming through the solution outside the micelles. Finally, the size of the nanoparticle exceeds that of the initial water core, and the particle growth stops when a certain size is reached—in the thermodynamic control—or when the nutrient is exhausted—in the case when the LaMer diagram is followed (5°). The nanoparticle is stabilized by a layer of

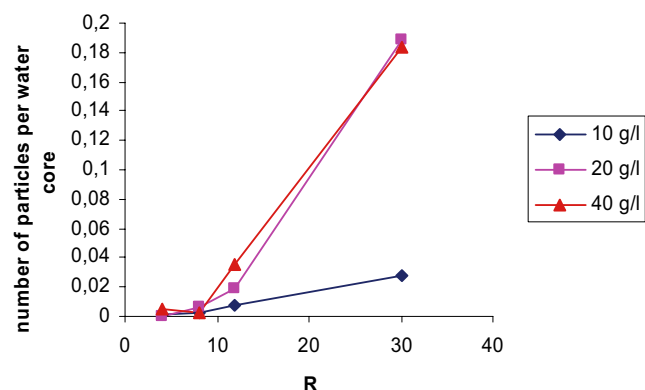


Fig. 4 Variation of the number of nanoparticles formed per water core as a function of R for various concentrations of retinol

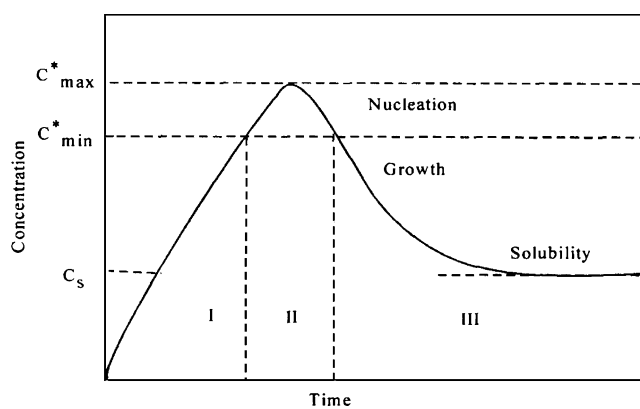
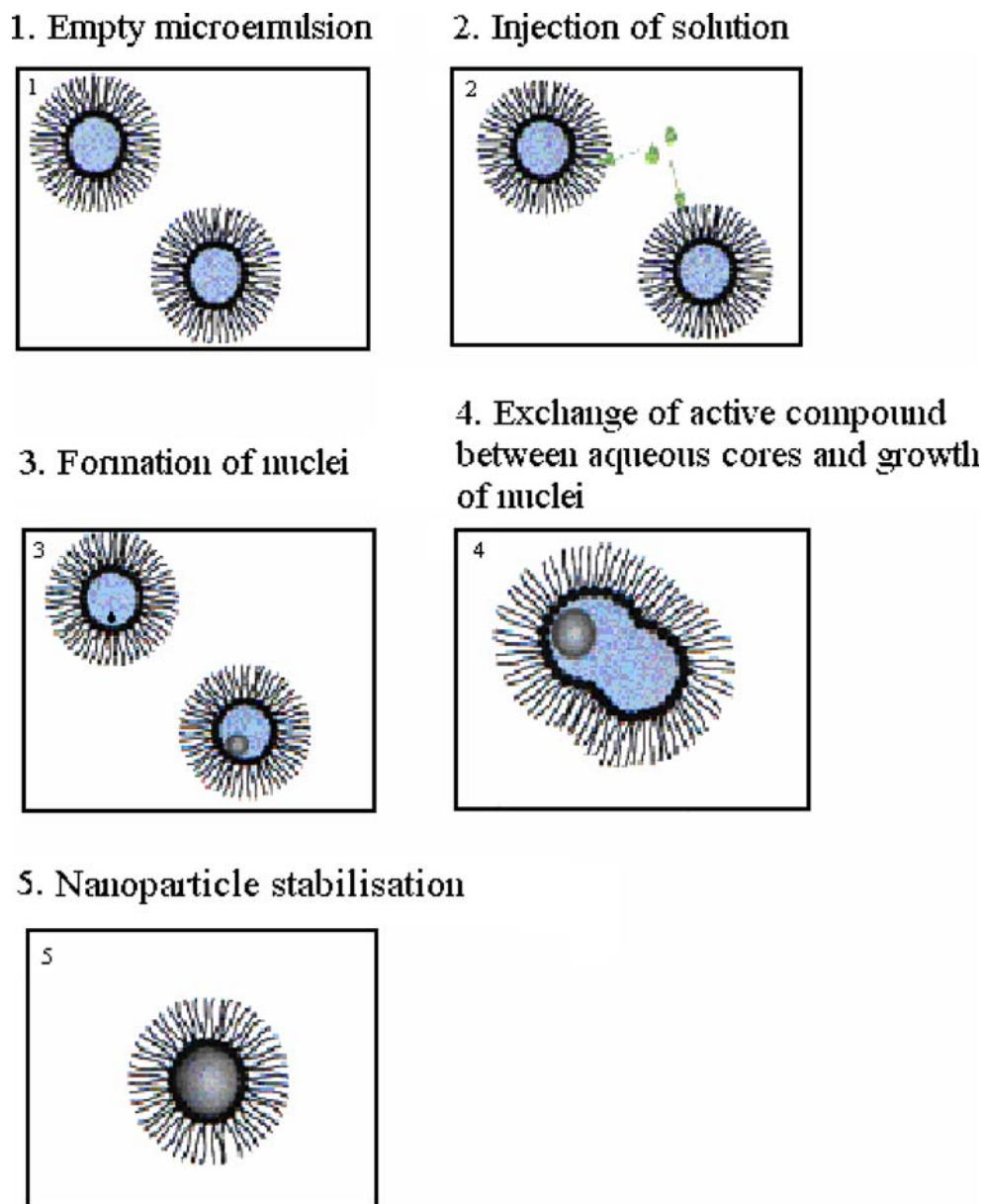


Fig. 5 LaMer diagram for precipitation reaction

Fig. 6 Mechanism of formation of the organic nanoparticles in microemulsions



surfactant, the polar head groups of the surfactant are hydrated, and a part of the vector solvent is also included at the interface (see below).

Properties of the nanoparticles

The J-complex

The optical properties of molecular aggregates differ strongly from single molecules and pure crystals. Electrostatic intermolecular interactions in the aggregate couple optical transitions on different molecules. In general, the strength of this coupling depends on the size of the transition dipole moment, the relative orientation of the molecules, and

the intermolecular distances. Through this coupling, an optical excitation on a particular molecule can be transferred to other molecules in the aggregates, that is, the

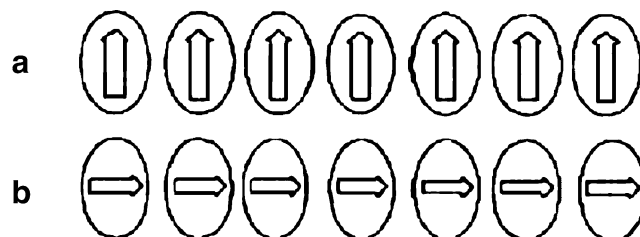


Fig. 7 **a** Unfavorable arrangement between the transition dipole moments: H-aggregate; **b** favorable arrangement between the transition dipole moments: J-aggregate

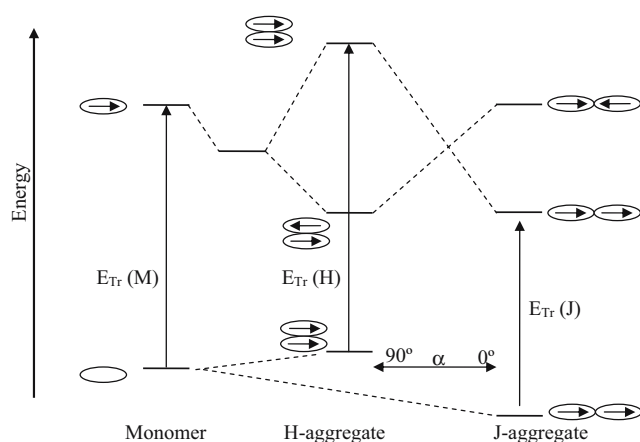


Fig. 8 Electronic transitions in the monomer, [E(M)], in the complexes J and H [E(J) and E(H)]. α is the angle formed between the transition dipole moment and the aggregate axis

excitation becomes delocalized. The timescale of this transfer is related to the coupling strength. If the excitation transfer occurs on a much faster timescale than other dynamical processes, such as dephasing of the optical transition and spontaneous emission, it will occur coherently, and the eigenstates are best described as collective states of a part of the aggregate [6].

The bathochromic or hypsochromic shift of the exciton band with respect to the absorption of the monomer can be understood on the basis of electrostatic interactions. As the wavelength of light is longer than the molecular spacing, its electric field has the same phase over a large number of molecules. Therefore, it stimulates a whole domain of transition dipoles to move in phase [26]. This is only possible if the transition dipoles have a parallel arrangement. The arrangement of dipoles of Fig. 7a is energetically unfavorable; the allowed absorption energy is at higher frequency than that of the isolated molecule: This is called the H-aggregate. Oppositely, when the arrangement of dipole is favorable (Fig. 7b), the absorption energy of the allowed transition is at lower frequency than that of the isolated molecule: This is the J-complex.

The molecular organization in an aggregate defines the type of aggregate. If the angle, α , between the transition dipole moment and the aggregate axis is greater than 54.7° , an H-aggregate is formed, while for $\alpha < 54.7^\circ$, one obtains a J-aggregate. Figure 8 illustrates the various electronic transitions in J- and H-aggregates [27]. Note that arrows in the ground state represent the permanent dipole moments, while those in the excited state represent the transition dipole moments.

It has to be added that the line width of the excitonic transition decreases with the number of molecules in the aggregate due to an exchange narrowing effect. The quickly moving exciton is subject only to an average inhomogeneity which is reduced by roughly a factor of \sqrt{N} , where N is the number of coherently coupled molecules [27].

Hence, it is possible to calculate the number of molecules per aggregate (N), for example in the case of a linear aggregate:

$$\cos \left[\frac{\pi}{(N+1)} \right] = \frac{\Delta v_N}{\Delta v_\infty}$$

where $\Delta v_N = v_{\text{monomer}} - v_{J\text{-complex}}$, the bathochromic shift of the J-complex with respect to the monomer and Δv_∞ is the bathochromic shift for an infinite chain $\Delta v_\infty = v_{\text{monomer}} - v_\infty$ [28].

Another method can be used to compute the number of molecules per aggregate. This method is related to the FWHH [29]:

$$\frac{\Delta v_{1/2}(M)}{\Delta v_{1/2}(J(N))} = N^{1/2}$$

where $\Delta v_{1/2}(M)$ is the band width of the monomer and $\Delta v_{1/2}(J)$ is the band width of the J-complex containing N coupled molecules.

J-complex formed by retinol

The UV-visible spectra of monomeric retinol in n-heptane and of retinol nanoparticles in the microemulsion with $R=$

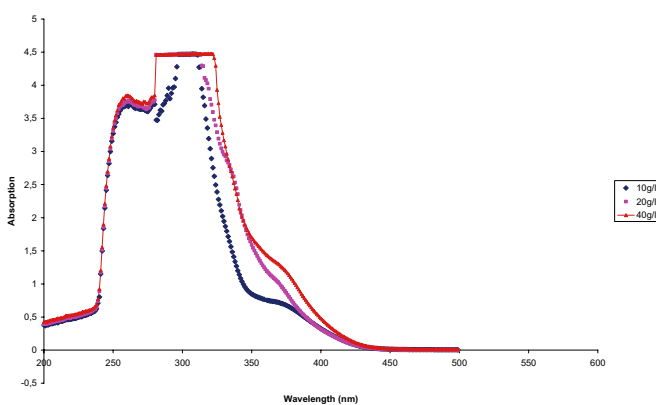
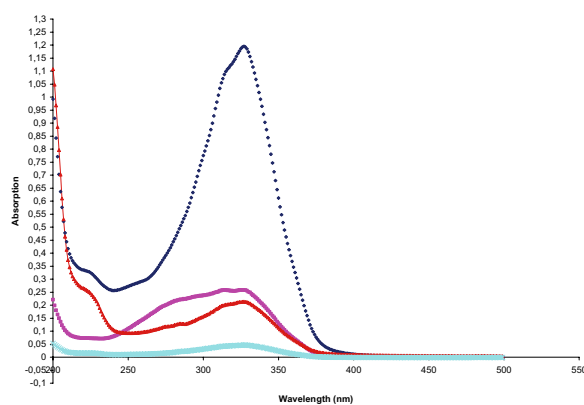


Fig. 9 UV-visible spectra of retinol in n-heptane (a) and the spectra of retinol nanoparticles in microemulsion with $R=12$ (b)

Table 2 UV-visible spectral characteristics of retinol nanoparticles

| <i>R</i> | C_v^a (g/l) | λ_{max} (nm) | $1/\lambda_{max}$ (cm^{-1}) | $\nu_M - \nu_{max}$ (cm^{-1}) | $\Delta\nu_{1/2}$ (cm^{-1}) |
|----------|------------------|-------------------------|------------------------------------|--------------------------------------|------------------------------------|
| 4 | 40 | 374 | 26,740 | 4,030 | 3,590 |
| 8 | 10 | 378 | 26,460 | 4,310 | 3,900 |
| | 20 | 353 | 28,330 | 2,440 | 4,850 |
| | 40 | 366 | 27,320 | 3,450 | 4,360 |
| 12 | 10 | 368 | 27,170 | 3,600 | 4,080 |
| | 20 | 355 | 28,170 | 2,600 | 4,800 |
| | 40 | 365 | 27,400 | 3,370 | 4,150 |

^a C_v (g/l), concentration of retinol with respect to chloroform

12 are reported in Fig. 9. It is clearly seen that a new band appears at ca 360 nm, while the maximum of the monomer is at ca 325 nm.

The various UV-visible spectra of the retinol nanoparticles are decomposed as the sum of peaks and a linear background. The line shape was chosen to be a linear combination of a Gaussian and a Lorentzian function,

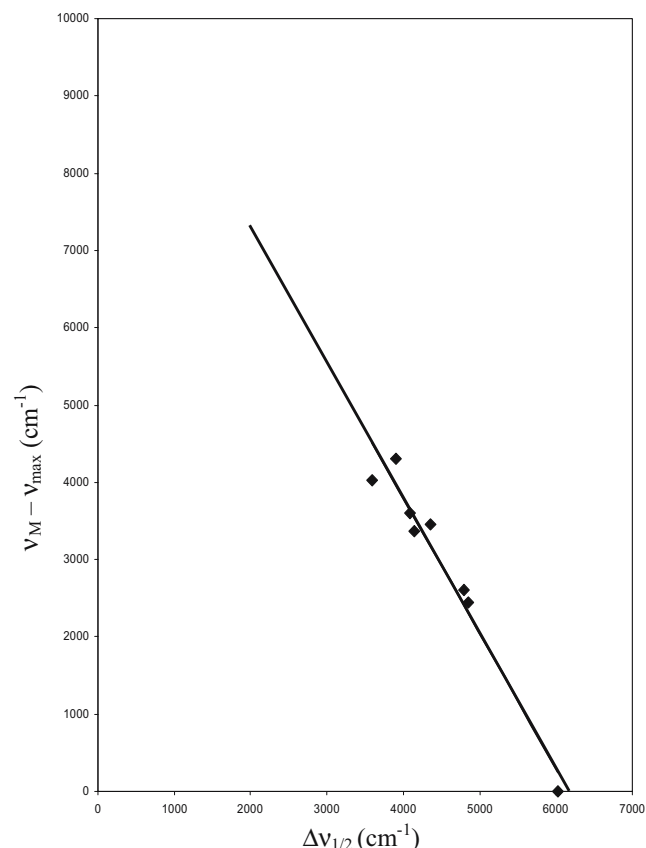


Fig. 10 Variation of the bathochromic shift of the J-complex, $\Delta\nu_N = \nu_M - \nu_{J-complex}$ and the band width at half maximum $\Delta\nu_{1/2}$

having an equal contribution of Gaussian and Lorentzian functions, in an attempt to reproduce the influence of instrumental factors on the natural line shape. In the first step, the number of peaks and the relevant parameters (position, width, and height) were estimated by inspection of the data. These initial values were then improved upon by a least-square method.

Table 2 gives the λ_{max} values in nanometer, the wave numbers in cm^{-1} , the difference $\nu_M - \nu_{J-complex}$ (the bathochromic shift) in cm^{-1} , and FWHM.

Retinol molecules form a J-type complex by aggregation because the excitonic band in the UV-visible region of the spectrum is bathochromic with respect to the monomer absorption band (Fig. 9). From the variation of the maxima of the absorption band and the bandwidths of the absorption band, the number of coupled monomers per J-complex can be computed [28, 29]. Figure 10 illustrates the variation of $\Delta\nu_N = \nu_M - \nu_{J-complex}$ as a function of the bandwidth at half maximum $\Delta\nu_{1/2}$. We find $\nu_M = 30,770\text{ cm}^{-1}$ and $\Delta\nu_{1/2}(M) = 6020\text{ cm}^{-1}$. The correlation is quite linear, the bathochromic effect increases with decreasing band width, characteristic of the excitonic band. Indeed, the larger the excitonic domain, the faster the excitation transfer from one molecule to the other, hence, smaller will be the bandwidth.

If a bandwidth of ca $2,000\text{ cm}^{-1}$ is estimated for the largest J-complex, ν_∞ can be estimated to $23,770\text{ cm}^{-1}$ for a J-complex of infinite length.

From the bandwidth at half maximum the number of monomer in the J-complex, (N) is computed as:

$$\frac{\Delta\nu_{1/2}(M)}{\Delta\nu_{1/2}(J)} = N^{1/2}$$

The so-obtained values vary between 1.5 and 2.8, meaning that the J-complex is formed between two and three molecules.

Assuming a linear aggregate, the N value can also be computed from the variation of ν_{max} :

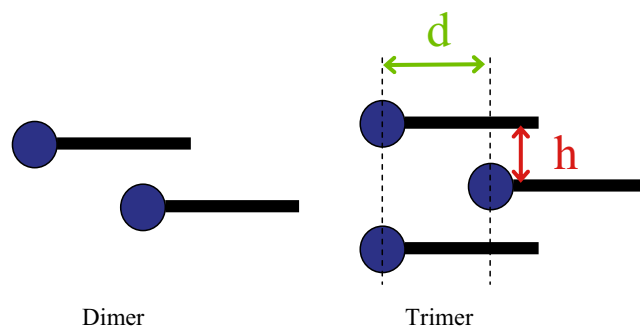



Fig. 11 Schematic representation of a head-to-tail retinol ladder aggregate with two parameters: d the sliding parameter and h the intermolecular distance

Table 3 Effect of d parameter on the spectral characteristics of retinol in J-complex: ν_{\max} and oscillator strength in parenthesis for $h=5.0$ Å

| Head-to-tail |  | | | |
|--------------|---|------------|------------|------------|
| | $d=5.0$ Å | $d=6.0$ Å | $d=7.0$ Å | $d=8.0$ Å |
| 328 (1.75) | 364 (0.83) | 344 (0.74) | 336 (0.29) | 357 (1.20) |
| | 330 (0.04) | 327 (0.40) | 326 (3.54) | 329 (3.74) |
| | 321 (4.12) | 324 (3.82) | 324 (1.25) | 332 (0.14) |
| $S^a=5.25$ | $S=4.99$ | $S=4.96$ | $S=5.08$ | $S=5.08$ |

^a S is the sum of oscillator strength.

$$\cos \left[\frac{\pi}{(N+1)} \right] = \frac{\nu_M - \nu_J}{\nu_M - \nu_\infty}$$

where ν_∞ is the ν_{\max} of a J-complex of infinite length. Note that this method also yields N values varying between two and three molecules.

As a conclusion, the nanoparticles of retinol containing between 100 and 1,000 molecules are formed of J-aggregates separated by molecules the orientation of which cannot fit the J-complex. Indeed, the most probable structure of the J-complex is a ladder form for the trimer and for the dimer, the retinol molecules have to maintain the same direction of the dipole moment. Indeed, as the excitation wavelength is much larger than the size of the aggregate, only those molecules which are in-phase can be excited, leading to a bathochromic shift (Fig. 11).

In both aggregates, the stabilization can occur when the monomers are in a shifted position.

One point could be further developed concerning the formation of a first nucleus. It is possible that the first

nucleus could be just the J-complex, the presence of which should be detectable using fast kinetic methods.

Dye molecules could also be adsorbed on silver halide nanoparticles, and in these cases, the number of molecules per J-complex could be higher than three [7–11]. The stationary and time-resolved fluorescence spectra indicate a quenching effect of the dye fluorescence by the particles suggesting that dye molecules could be suitable for the spectral sensitization [10]. Oppositely, an enhanced excitonic fluorescence of J-aggregates of dye molecules was observed on 12 nm gold particles by Tian et al. [30].

Quantum chemical computation on the J-aggregates

The quantum chemical study gives further information on the relationship between the structure of the J-complex and their UV-visible spectra. Figure 11 lists a schematic representation of a head-to-tail ladder aggregate of retinol. Table 3 gives the computed values of the (vertical) excitation energy and the oscillator strength for each band

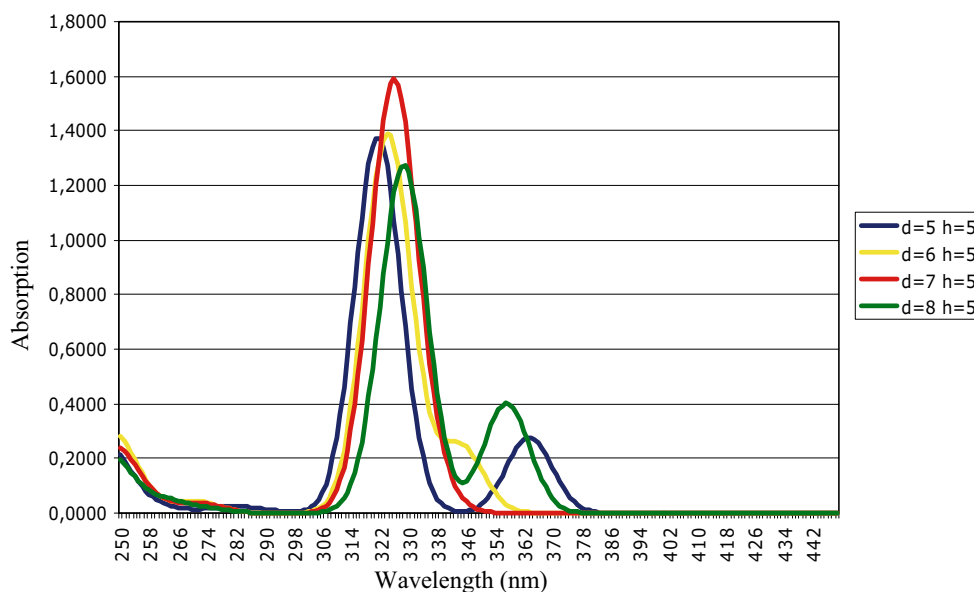
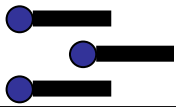
Fig. 12 Simulated UV-visible spectra of the monomer and excitonic bands as a function of the sliding parameter d for $h=5.0$ Å

Table 4 Effect of h parameter on the spectral characteristics of retinol in J-complex: ν_{\max} and oscillator strength in parenthesis for $d=6.0$ Å

| Head-to-tail |  | | |
|-------------------------|--|--|--|
| | $h=6.0$ Å | $h=5.0$ Å | $h=4.5$ Å |
| 328 (1.75) | 328 (0.01) 327 (0.01) 321 (5.35) | 344 (0.74) 327 (0.40) 324 (3.82) | 510 (0.12) 384 (0.77) 359 (0.05) 328 (1.40) 326 (1.21) 324 (0.39) 293 (1.03) |
| $S_{\text{total}}=5.25$ | $S=5.37$ | $S=4.96$ | $S=4.97$ |

as well as the total oscillator force as a function of the horizontal displacement, d (in Å) for $h=5.0$ Å. This parameter is important because the retinol molecule is not planar; indeed, a solid angle of ca 60° is formed between the olefinic chain and the cycle [31]. As a consequence, the optimized value is close to 5.0 Å.

The UV-visible spectra of the J-complex were also simulated to show the new excitonic band. Figure 12 illustrates the UV-visible spectra of the monomer and the excitonic bands for various d values for $h=5.0$ Å. For $d=5.0$ Å, a new bathochromic band appears at ca 362 nm. For $d=6.0$ Å, the bathochromic effect is less pronounced and only a shoulder appears. For $d=7.0$ Å, the excitonic band is not resolved, while for $d=8.0$ Å, it reappears at ca 355 nm. This emphasizes the role of the methyl groups in the side

chain of the molecule, leading to various types of intramolecular interactions depending on the d value. Note that the spectra for $d=6.0$ Å reproduces approximately the experimental results (Fig. 9).

The influence of the intermolecular distance h is illustrated in Table 4, and Fig. 13 shows the corresponding spectra for $d=6.0$ Å. The experimental spectra are approximately reproduced for $h=5.0$ Å (Fig. 13), while for h values larger than 6.0 Å, no new excitonic band could be obtained.

As some 100–1,000 retinol molecules form a nanoparticle (Table 1), it is also interesting to consider the aggregation of more than three molecules in the J-complex. Table 5 gives the excitation energies of the UV-visible absorption band for head-to-tail ladder aggregates formed

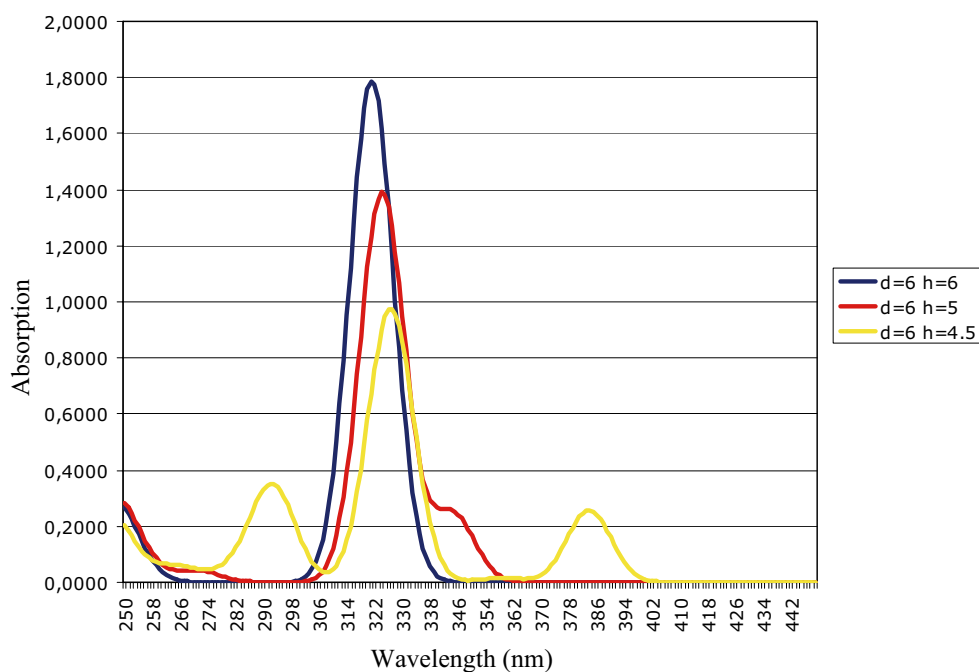




Fig. 13 Simulated UV-visible spectra of the monomer and excitonic bands as a function of the intermolecular distance h for $d=6.0$ Å

Table 5 Effect of the number of retinol molecules in head-to-tail configurations for $d=6.0$ Å and $h=5.0$ Å

| | | | |
|---|---|---|---|
|  |  |  |  |
| AB | ABA | ABAB | ABABA |
| 327 (0.07) | 344 (0.74) | 343 (0.71) | 346 (0.01) |
| 325 (3.43) | 327 (0.40) | 329 (0.002) | 339 (1.56) |
| | 324 (3.82) | 325 (0.14) | 328 (0.003) |
| | | 322 (5.86) | 325 (0.27) |
| | | | 321 (6.44) |
| $S/2 = 1.75$ | $S/3 = 1.65$ | $S/4 = 1.68$ | $S/5 = 1.65$ |

of dimer (AB), trimer (ABA), quadrimer (ABAB), and pentamer (ABABA). Figure 14 illustrates the corresponding spectra. It is important to note that aggregates including more than three molecules do not change significantly the UV-visible spectra. As a conclusion, a trimer contains most of the signature of a J-complex, and the theoretical investigation confirms the experimentally determined J-complex composition.

To complete the study, the possible formation of tail-to-tail ladder aggregates was also considered. Table 6 and Fig. 15 illustrate the excitation energies of the UV-visible spectra and their oscillator strength as well as the UV-visible spectra. It is important to see that in these cases, no new bathochromic band appears in the spectra (Fig. 15).

Finally, the effect of mixing the retinol molecules in an aggregate composed of both head-to-tail and tail-to-tail

Fig. 14 Simulated UV-visible spectra of head-to-tail dimer (AB), trimer (ABA), quadrimer (ABAB), and pentamer (ABABA) of retinol molecules with $d=6.0$ Å and $h=5.0$ Å

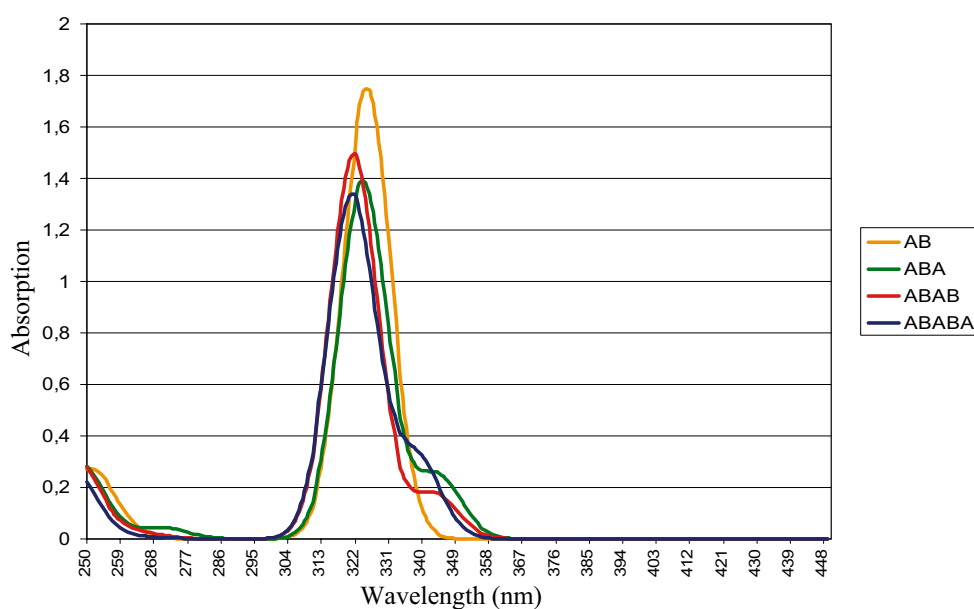


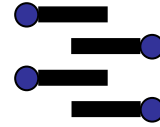
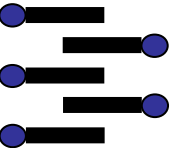


Table 6 Effect of the number of retinol molecules in tail-to-tail configurations for $d=6.0$ Å and $h=5.0$ Å

| | | | |
|---|---|--|---|
|  |  |  |  |
| AJ | AJA | AJAJ | AJAJA |
| 326 (3.48) | 329 (0.07) | 321 (6.99) | 330 (0.04) |
| centrosymmetrical | 325 (0.69) | centrosymmetrical | 325 (0.06) |
| | 321 (4.52) | | 322 (0.36) |
| | | | 319 (8.29) |
| $S/2 = 1.74$ | $S/3 = 1.76$ | $S/4 = 1.75$ | $S/5 = 1.75$ |

ladder configurations was also studied because in principle, all the configurations could occur in a nanoparticle. The results are reported in Table 7 for tetramers and heptamers. Figure 16 illustrates the UV-visible spectra of the aggregates containing three molecules associated in a head-to-tail ladder configuration. It can be seen that this configuration dominates all the shape of the spectra whatever the number of the retinol molecules in the aggregates. These results confirm, once again, the presence of head-to-tail trimers forming the J-complex (Table 7).

Characterization of cholesterol nanoparticles by ^2H -NMR

As the retinol nanoparticles were not characterized yet by ^2H -NMR techniques, we take the assumption that the two types of nanoparticles would behave similarly, as it was already shown for other related organic nanoparticles [32].

First, the influence of the temperature on the state of the water in the cores of the empty microemulsions is studied. The study of the water in the microemulsions containing only the solvent and also in microemulsions containing

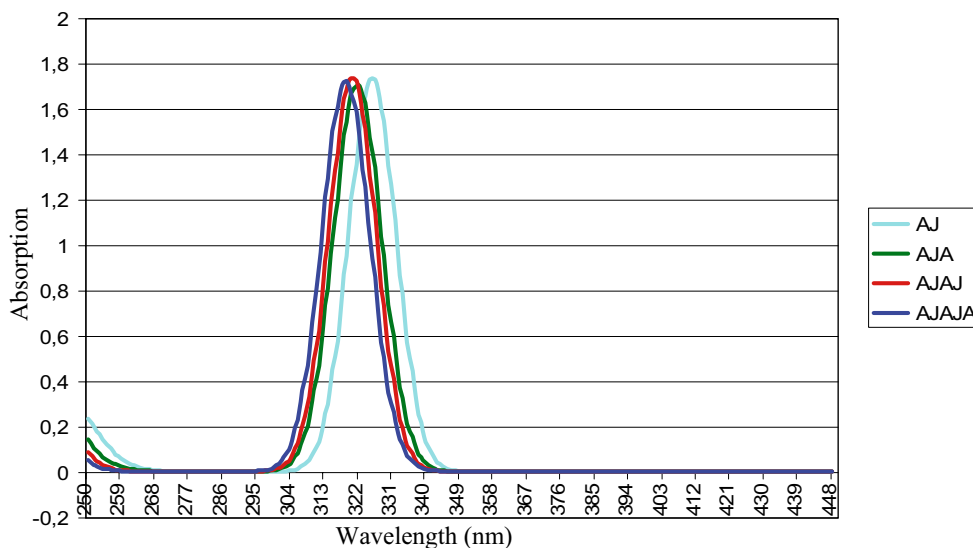
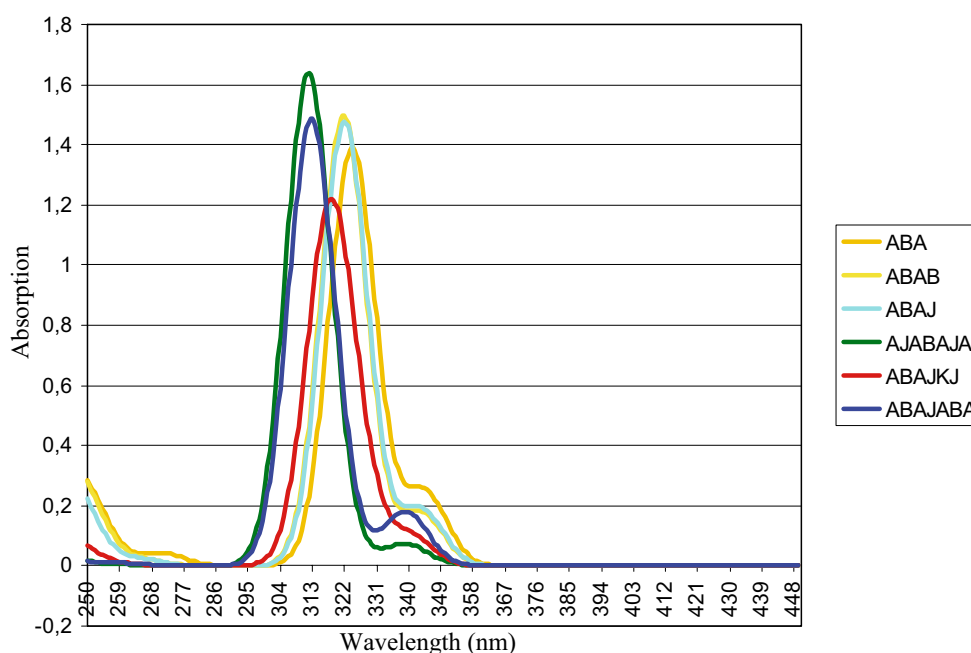
Fig. 15 Simulated UV-visible spectra of tail-to-tail dimer (AJ), trimer (AJA), quadrimer (AJAJ), and pentamer (AJAJA) of retinol molecules with $d=6.0$ Å and $h=5.0$ Å

Fig. 16 Simulated UV-visible spectra of mixed aggregates of trimers, quadrimers, and heptamers of retinol molecules with $d=6.0$ Å and $h=5.0$ Å



nanoparticles is carried out. Two values (4 and 1) were selected for the R factor ($R=[\text{H}_2\text{O}]/[\text{AOT}]$) of the studied microemulsions. This factor is related to the size of the aqueous core. The reference is pure deuterated water. The ^2H -NMR spectra of different microemulsions are represented in Fig. 17 for the empty microemulsions ($R=1$; a), the one containing chloroform and cholesterol nanoparticles (b).

Two types of NMR lines are observed at room temperature. The first one is located at -0.86 ppm. This stems from the free molecules of water and from water molecules bound to the surfactant. Hydrogen bonds characterize these states of water, and hence, the chemical shift occurs at lower fields. For lower R values, the shift corresponds to the bound water molecules which interact with the surfactant polar group and with the counterion Na^+ . The second and third lines are due to the water molecules as monomers or dimers. These are located at higher fields (-3.65 and -4.04 ppm, respectively) because only a small amount of hydrogen bonds are present. The water molecules also interact with the surfactant. These molecules are trapped at the interface.

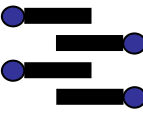
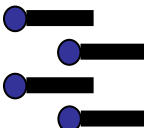
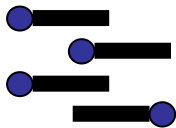
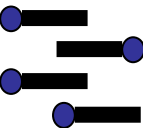
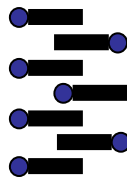
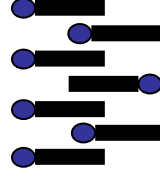
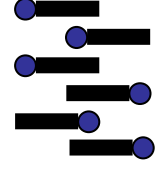
Generally, three kinds of water may exist in a microemulsion medium: “bulk” water in the center of the water core; “bound” water, which interacts with the hydrophilic part of the surfactant molecule; and “trapped” water, which is trapped in the interface in the form of monomers or dimers [33]. Bulk water molecules are normally not present for R values below 6–10 where all the water molecules are structured because of their interaction with Na^+ counterions and the strong dipole of the AOT polar group [34]. In this case, where the ratio R is equal to 1, only two kinds of

water molecules should be expected. Therefore, it is assumed that the two NMR lines observed here correspond to bound water and to trapped water. To check this assumption, the same experiment was repeated for higher R values in which case the chemical shift increases with the R value until reaching approximately that of pure deuterated water (used as reference), while the FWHM decreases with increasing R values.

This variation has already been observed [34] and is the result of a fast exchange (faster than $2 \times 10^{10} \text{ s}^{-1}$) between bulk and bound water. At low R values, the observed chemical shift comes from the variation of the number of hydrogen bonds in which the water molecules are involved. In fact, the water molecules adsorbed at the interface (or solvating the Na^+ ions) form fewer hydrogen bonds, provoking a high-field chemical shift. This decreasing number of hydrogen bonds has previously been observed by Wong et al. [35] using ^1H NMR experiments.

The microemulsions are stable as a function of temperature. When the temperature decreases, the intensity of the line decreases, and it broadens until it finally vanishes (Fig. 17). The solidification of the water occurs at 253 K in the empty microemulsions and at 243 K in the other two cases, while pure water solidifies at 273 K. These values cannot be compared with those obtained in microemulsions with low R . Indeed, the decrease in the line of free water stems from two factors: the solidification of the water and the increase in the bound water. There is no significant shift of the NMR lines. The other two lines of the trapped water do not significantly change: Their location (light shift towards low fields) and width stay constant.

Table 7 Effect of the number of retinol molecules in mixed head-to-tail and tail-to-tail configurations for $d=6.0$ Å and $h=5.0$ Å

| | | | |
|--|--|---|---|
|  |  |  |  |
| Tail-to-tail | Head-to-tail | | |
| AJAJ | ABAB | ABAJ | AJAB |
| 321 (6.99) | 343 (0.71) | 343 (0.76) | 329 (0.002) |
| | 329 (0.002) | 329 (0.01) | 328 (0.01) |
| | 325 (0.14) | 325 (0.20) | 322 (0.001) |
| | 322 (5.86) | 322 (5.72) | 320 (7.01) |
| S = 6.99 | S = 6.81 | S = 6.68 | S = 7.02 |
| | | Idem head-to-tail | Idem tail-to-tail |
|  |  |  | |
| AJABAJA | ABAJABA | ABAJKJ | |
| 339 (0.50) | 339 (0.66) | 340 (0.72) | |
| 324 (0.07) | 339 (0.59) | 324 (1.94) | |
| 322 (0.02) | 324 (0.10) | 317 (7.37) | |
| 319 (0.02) | 320 (0.01) | | |
| 318 (0.25) | 318 (0.66) | | |
| 316 (0.03) | 313 (9.89) | | |
| 312 (11.26) | | | |
| S = 12.15 | S = 11.91 | S = 10.03 | |

From these results, it can be seen that the presence of the nanoparticles or the solvent in the microemulsions does not significantly influence the nature of the water. Hence, the nanoparticles should be located in the organic phase and

not in the aqueous cores. The other reason for localizing the nanoparticles in the organic phase is that the diameter of the nanoparticles (5.0 nm) is greater than the aqueous cores size ($R=1$; $d=1.26$ nm), and it is, thus, impossible to locate

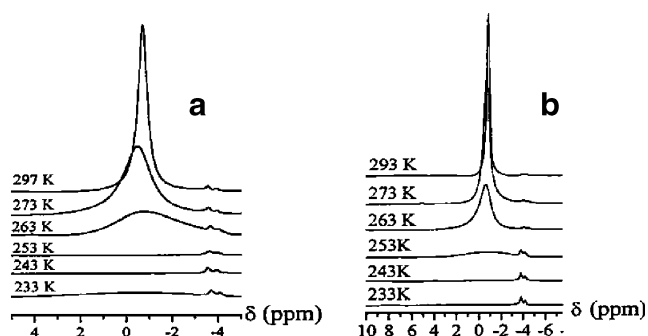


Fig. 17 ^2H -NMR spectra of water in microemulsions ($R=1$) **a** empty; **b** with solvent chloroform and nanoparticles of cholesterol as a function of temperature

the nanoparticles inside the aqueous cores. On the other hand, some water could be adsorbed on the nanoparticles. Another hypothesis is that the vector solvent could be in the organic phase or adsorbed on the nanoparticles, but not in the aqueous cores.

The aim was to determine the location of the solvent chloroform. Different spectra have been compared: pure CDCl_3 , CDCl_3 in heptane, and CDCl_3 in heptane/AOT solution. The first line stands for the associated CDCl_3 at 2.40 ppm (pure CDCl_3) and 2.66 ppm for CDCl_3 in heptane or in heptane/AOT solution. The two small lines at -3.18 and -3.58 ppm (higher fields), in the case of CDCl_3 in heptane and in heptane/AOT solution, stand for CDCl_3 dimers or monomers. In the microemulsions, the lines are situated at the same position. The line at lower fields has almost the same chemical shift as those obtained in heptane/AOT solution. Thus, the CDCl_3 molecules should solvate the polar head group of AOT and should be in contact with the aqueous cores.

The study of the influence of the temperature on the CDCl_3 in microemulsions (empty or with nanoparticles) is also carried out. The high-intensity lines (due to associated CDCl_3) decrease as a function of temperature in the two cases. In the presence of the nanoparticles, the intensity is smaller, and the line is broader at 233 K compared to those without nanoparticles. The hypothesis is that the CDCl_3 would be adsorbed on the nanoparticles. Indeed, the width of the lines is inversely related to T_2^* (transversal relaxation time). Thus, when the width increases, the relaxation time decreases, and the molecules are more frozen. The other two lines at higher fields (due to monomers or dimers) do not significantly change as a function of the temperature.

As a conclusion, the chemical shift is independent of the presence of the nanoparticles. Some water is adsorbed on the nanoparticles, in addition to the surfactants. Secondly, NMR measurements of deuterated chloroform show that it is adsorbed on the nanoparticles. The NMR spectra allow one to conclude that the nanoparticles are essentially stabilized in

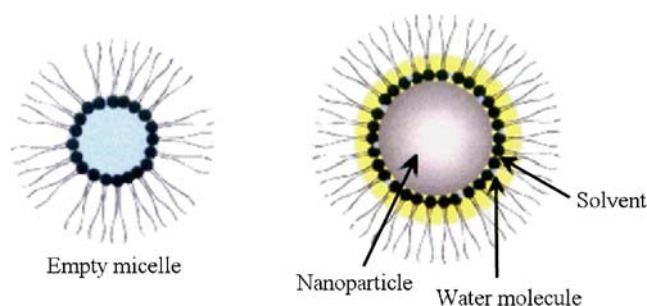


Fig. 18 General picture of the stabilization of the nanoparticles prepared from the microemulsion

the organic phase with solvent, and surfactant molecules (water, chloroform, and AOT) adsorbed on them (Fig. 18).

Conclusions

Quasi monodisperse nanoparticles of retinol can be easily prepared by precipitating them in the inner water cores of microemulsions. These water cores behave thus like nano-reactors. The size of the nanoparticles does not depend much either on the R value or the concentration of retinol. This is explained by the thermodynamic stabilization of nanoparticles of a certain size. The transport of the retinol molecules through the organic phase and the interface is facilitated by the solvent vector chloroform. The so-formed nanoparticles are stabilized by the adsorbed surfactant molecules. It could be shown also that some water and some chloroform were also adsorbed on the nanoparticles.

The retinol molecules form J-complexes by associating head-to-tail ladders in the aggregates. The existence of the J-complex is demonstrated by the bathochromic shift of the UV-visible spectra to the monomers. In addition, the bandwidth of the excitonic band decreases with increasing bathochromic shift. From the experimental data, it is possible to calculate the number of retinol molecules organized in the form of J-complex, which is found to be in the two to three range.

The quantum chemical calculations confirm the presence of J-complexes. Their configuration is head-to-tail, and three molecules are sufficient to confer to the J-complex their absorption signature. This trimer gives the fundamental properties of the J-complex whatever the relative orientation of the other molecules of the aggregates.

Acknowledgment C. Destrée gratefully acknowledges financial support from FRiA, Belgium. B. Champagne thanks the Belgian National Fund for Scientific Research for his Research Director position. The calculations have been performed on the Interuniversity Scientific Computing Facility (ISCF), installed at the Facultés Universitaires Notre-Dame de la Paix (Namur, Belgium), for which the authors gratefully acknowledge the financial support of the FNRS-FRFC and the “Loterie Nationale” for the convention no. 2.4578.02 and of the FUNDP. J. Ghijsen thanks the Belgian National Fund for Scientific Research for his Research Associate position.

References

- Fendler JH (ed) (1998) Nanoparticles and nanostructured films: preparation, characterization and applications. Wiley-VCH, Weinheim
- Destrée C, B.Nagy J (2006) *Adv Colloid Interface Sci* 123–126:353
- Ozin GA, Kuperman A, Stein A (1989) *Angew Chem Int Ed Engl Suppl* 28:359
- Belloni J, Mostafavi M, Marignier J-L, Amberad J (1991) *J Imaging Sci Technol* 35:68
- Henglein A (1993) *J Phys Chem* 97:5457
- Kobayashi T (ed) (1996) *J-Aggregates*. World Scientific, Singapore
- Jeunieu L, B.Nagy J (1998) *Appl Organomet Chem* 12:341
- Jeunieu L, B.Nagy J (1999) *Nanostruct Mater* 12:979
- Jeunieu L, B.Nagy J (1999) *Colloids Surf A Physicochem Eng Asp* 151:419
- Jeunieu L, Verbourwe W, Els Rousseau, Van der Auweraer M, B.Nagy J (2000) *Langmuir* 16:1602
- Jeunieu L, Alin V, B.Nagy J (2000) *Langmuir* 16:597
- Jeunieu L, Debuigne F, B.Nagy J (2001) Reaction and synthesis in surfactant systems. In: Texter J (ed) *Surfactant science series*, vol 100. Marcel Dekker, New York, p 609
- Zerner MC (1991) In: Lipkowitz KB, Boyd DB (eds) *Reviews of computational chemistry*, vol 1. VCH, New York, 313
- Martin CH, Zerner MC (1999) In: Solomon EI, Lever ABP (eds) *Inorganic electronic structure and spectroscopy*, vol 1. Wiley, New York, p 555
- Guillaume M, Botek E, Champagne B, Castet F, Ducasse L (2002) *Int J Quantum Chem* 90:1378
- Guillaume M, Botek E, Champagne B, Castet F, Ducasse L (2004) *J Chem Phys* 121:7390
- Eastoe J, Robinson BH, Visser AJWG, Steatler DC (1987) *Faraday Trans* 87:1899
- Landolt-Börnstein (1985) New series, vol 106. Springer, Berlin Heidelberg New York, p 166
- Fletcher PDI, Howe AM, Robinson BH (1987) *J Chem Soc Faraday Trans I* 83:985
- Atik SS, Thomas JK (1981) *Chem Phys Lett* 79:351
- LaMer VK, Dinegarn RH (1950) *J Am Chem Soc* 72:4847
- Sugimoto T (1987) *Adv Colloid Interface Sci* 28:65
- B.Nagy J (1999) In: Kumar P, Mittal KL (eds) *Handbook of microemulsion science and technology*. Marcel Dekker, New York, p 499
- Lerot L, Legrand F, De Bruycker P (1991) *J Mater Sci* 26:2353
- Destrée C, Ghijsen J, B.Nagy J (2007) *Langmuir* 23:1965
- Pope M, Swenberg CE (1999) *Electronic processes in organic crystals and polymers*. Oxford University Press, Oxford
- Sherer POJ (1996) In: Kobayashi T (ed) *J-Aggregates*. World Scientific, Singapore, p 95
- Moll J (1995) *Forschungsbericht* 214: exciton-dynamics in J-aggregates of an organic dye. Bundesanstalt für Materialforschung und-prüfung, Berlin
- Knapp EW (1984) *Chem Phys* 85:73
- Tian Y, Guerin F, Guldi D, Fendler JH (1996) Nanoparticles in solids and solutions. In: Fendler JH, Dekany I (eds) *NATO ASI Series*, 3. High technology, vol 18. Kluwer, Dordrecht, p 569
- Becker RS, Berger S, Dalling DK, Grant DM, Pugmire RJ (1974) *J Am Chem Soc* 96:7008
- Debuigne F (2002) PhD Thesis, University of Namur
- Jain TK, Varshney M, Maitra A (1989) *J Phys Chem* 93:7409
- Hauser H, Gaering G, Pande A, Luisi PL (1989) *J Phys Chem* 93:7869
- Wong M, Thomas JK, Novak T (1977) *J Am Chem Soc* 99:4730